Numerical Study of Turbulent Flow and Heat Transfer in A Novel Design of Serpentine Channel Coupled with D-Shaped Jaggedness Using Hybrid Nanofluid

Submitted By

RM Raditun Elahe Ratul

180011126

Supervised By

Dr. Arafat Ahmed Bhuiyan

A Thesis submitted in partial fulfillment of the requirement for the degree of Bachelor of Science in Mechanical Engineering

Department of Mechanical and Production Engineering (MPE)

Islamic University of Technology (IUT)

19th May 2023

Candidate's Declaration

This is to certify that the work presented in this thesis, titled, "**Numerical study of turbulent flow and heat transfer in a novel design of serpentine channel coupled with D-shaped Jaggedness using Hybrid nanofluid**", is the outcome of the investigation and research carried out by me under the supervision of **Dr. Arafat Ahmed Bhuiyan, PhD, Associate Professor, Department of Mechanical and Production Engineering, IUT.**

It is also declared that neither this thesis nor any part of it has been submitted elsewhere for the award of any degree or diploma.

RM Raditun Elahe Ratul
Student ID: 180011126

RECOMMENDATION OF THE BOARD OF SUPERVISORS

The thesis titled "**Numerical study of turbulent flow and heat transfer in a novel design of serpentine channel coupled with D-shaped Jaggedness using Hybrid nanofluid**" submitted by **RM Raditun Elahe Ratul**, Student ID: **180011126** has been accepted as satisfactory in partial fulfillment of the requirements for the degree of B Sc. in Mechanical Engineering on **19th May, 2023.**

BOARD OF EXAMINERS

---

1. ----------

   Dr. Arafat Ahmed Bhuiyan (Supervisor)
   Associate Professor
   MPE Dept., IUT, Board Bazar, Gazipur-1704, Bangladesh.

2. ----------

   Dr. Md. Rezwanul Karim
   Associate Professor
   MPE Dept., IUT, Board Bazar, Gazipur-1704, Bangladesh.

3 ----------

   Fahim Tanfeez
   Lecturer
   MPE Dept., IUT, Board Bazar, Gazipur-1704, Bangladesh.

Acknowledgment

Firstly, the author would like to express his utmost gratitude and indebtedness to his esteemed supervisor, Dr. Arafat Ahmed Bhuiyan, PhD, Associate Professor, Department of Mechanical and Production Engineering, IUT, for his, invaluable suggestions, unending guidance, and encouragement to the research work throughout the duration of the period. This research work was made possible, as well as a productive one, thanks to his unflagging assistance and counsel at every level.

The author would like to express his heartfelt appreciation and gratitude to Syeda Saiyara Asgari for her unwavering support and encouragement throughout the journey of completing this thesis work. In conclusion, the author would also like to express his sincerest thanks to Farid Ahmed, PhD student at North Carolina State University, USA for his insightful direction and guidance in the simulation part of this work.

RM Raditun Elahe Ratul

Abstract

This study aimed to examine numerically the effects of a dimpled surface over a mini-channel heat exchanger on the flow characteristics and heat transfer across a serpentine channel with a uniform rectangular cross-section. The dimples were arranged in parallel with a spanwise (y/d) distance of 3.125 and streamwise (x/d) distance of 11.25 along just one side of the serpentine channel's surface. Turbulent flow regime with Reynolds number ranging from $5x10^3$ to $20x10^3$ in the channel with surface modification was studied using water and various volume concentrations (φ = 0.1%, 0.33%, 0.75%, 1%) of Al_2O_3-Cu/water hybrid nanofluid as the coolant to achieve a three-step passive heat transfer enhancement. Applying the Finite Volume Method (FVM), RNG k-ε turbulence model, and a constant heat flux of $50kW/m^2$, simulations were run assuming the mixture of Al_2O_3-Cu nanoparticles homogenous using ANSYS 2020 R1. The second-order upwind approach is used for approximation of solution and discretization with SIMPLE pressure-velocity coupling. Taking heat transfer increment and pressure drop penalty into consideration, the dimpled serpentine channel provides a 147% improvement in thermal efficiency using water as the coolant, and the dimpled channel with 1% vol. Al_2O_3-Cu/water nanofluid enhanced thermal efficiency by a remarkable maximum of 267% at Re $5x10^3$. The study also indicates that thermal efficiency increased with an increasing volume concentration of the nanofluid and increment in thermal efficiency gradually decreased as the Re increased. Such kind of improvement in thermal performance is extremely desirable in the current era of powerful and compact electrical devices which need better cooling and have small space for a heat exchanger.

Table of Contents

List of Figures

List of Tables

Nomenclatures and Symbols

CFD	: Computational Fluid Dynamics
Re	: Reynolds number
FVM	: Finite Volume Method
TKE	: Turbulent Kinetic Energy
Pr	: Prandtl number
e/d	: Dimple depth to dimple diameter ratio
HTC	: Heat transfer coefficient
x/d	: Stream wise spacing
y/d	: Span wise spacing
PEC	: Performance Evaluation Criterion
TI	: Turbulent Intensity
Nu	: Nusselt number
v	: Velocity (m/s)
T	: Temperature (K)
Dh	: Hydraulic diameter
$\dot{Q}$	: Wall heat flux (W/m^2)
C_p	: Specific heat of fluid (J/kg K)
P	: pressure (N/m^2)
k	: Thermal conductivity ($W\ m^{-1}\ K^{-1}$)
μ	: Dynamic viscosity ($(Ns)/m^2$)
W	: Watt
vol. %	: volume concentration (%)
wt%	: weight concentration (%)
ΔP	: Pressure Drop
ρ	: Density
φ	: Volume fraction (%)

Subscripts

i, j, k	: tensor index
rs:	: Rough Surface
ss:	: Smooth Surface

nf:	: Nanofluid
bf:	: Base Fluid
bulk:	: Bulk
w:	: Wall
l:	: Flow direction
0	: Initial value
avg:	: Averaged
u, v, and w	: Velocity components along x, y, and z directions respectively

Chapter 1: Introduction

1.1 Background of the Study

By allowing for a more effective transfer of heat from one fluid to another, heat exchangers are an essential component of a wide variety of industrial processes and energy distribution networks. One of the designs that is used rather often is the serpentine heat exchanger, which has a flow route in the form of a serpentine for improved heat transfer properties. This section presents an overview of the background of the investigation on serpentine heat exchangers, emphasizing the relevance of the research as well as the rationale behind it.

It is very necessary to have effective heat transfer in order to maximize the utilization of energy and enhance the overall performance of heat exchangers. The serpentine heat exchanger design has a number of benefits, including the ability to fit into small spaces, rapid heat transfer rates, and a minimal pressure drop. Because of these qualities, it is well-suited for use in a wide variety of applications, including radiators in automobiles, air conditioning and refrigeration systems, power plants, and refrigeration units. It is essential to get a solid understanding of the fundamental characteristics and performance parameters of serpentine heat exchangers in order to improve the efficiency, dependability, and overall effectiveness of these exchangers in a variety of different sectors.

This study was motivated by the need to further investigate and enhance the performance of serpentine heat exchangers. Despite current understanding and use of this design, there is still room for progress in thermal efficiency, compactness, material selection, and production procedures. The goal is to improve the overall performance of serpentine heat exchangers and solve current issues in particular application areas by examining the underlying processes, flow dynamics, heat transfer characteristics, and optimizing the design parameters.

The relevance of the topic, as well as the impetus for the investigation of serpentine heat exchangers, is outlined in the context of the study. This study aims to contribute to the advancements and understanding of serpentine heat exchangers, ultimately improving their efficiency and effectiveness in a variety of industrial sectors by investigating the fluid flow and heat transfer characteristics, optimizing design parameters, and evaluating their performance in various applications.

1.2 Objectives of the Study

Serpentine channels as heat exchanger in compact machines and equipment and a topic of current focus. Though various researches have been done for improving the existing channels, still there are rooms for improvement by the modifications of serpentine channel which can significantly improve the performance of modern devices. Again, hybrid nanofluid is a recent concept which has not been applied much in serpentine channels by researchers. So, taking these aspects into consideration, the objectives of this study are-

- Designing a novel serpentine heat exchanger with and without Surface Modification.
- Obtaining the better performing channel by CFD simulation using water as coolant.
- Studying the better performing channel with different concentrations of a hybrid nanofluid and analyzing the trend of the thermal performances of the nanofluids.
- The ultimate goal of this study is to achieve a 3-step passive heat transfer enhancement system.

Chapter 2: Literature Review

One of the biggest technological challenges in industries is improving the thermal performance of various devices and machines. Effective cooling is extremely desirable for assuring reliable or stable thermal performance, which raises the need for creating energy-efficient solutions to promote appropriate heat transfer while keeping installation and maintenance costs low. Active and passive methods for improving heat transfer rates are quite popular in the industry. Active methods involve coolant pulsation, magnetic or electrostatic fields, etc. [1-3]. Active methods require more power, which can inconvenience industries. Passive methods are gaining popularity due to lower costs and maintenance. Passive heat transfer enhancements include using nanofluids, increasing surface area and fluid turbulence[4-6]. Increasing the length of the flowing channel by coiling or serpentining it, introducing dimples, fins, ribs, different types of protrusions, corrugations to increase surface roughness, inserting helical coiled wire, twisted tapes, etc. along the fluid flow direction are prominent passive methods for heat transfer enhancement[7-11]. Serpentine channels have innumerable applications in almost all engineering sectors and industries like nuclear sector, chemical industries, solar collector,

HVAC and refrigeration systems, thermal engineering and power plants etc. Due to the compact size, large heat transfer area and curvature effects serpentine channels are most ideal for the use as heat exchangers.

According to fluid dynamics dimples, protrusions, and other passive methods disrupt boundary layer formation[12, 13]. This increases channel turbulence and heat transfer. Attaching flow fields for circulation and recirculation to the wall repeatedly and increasing the effective surface area improve thermal performance [14, 15]. Again, the use of nanofluid in corrugated and crooked channels (helix-shaped, spiral, twisted, or serpentine-shaped) is a modern passive heat transmission method [16-20]. Many applications and the immense significance of diverse technical thermal devices using nanofluid have come from these researches [21-24]. Porous channels are also quite oftenly used as the heat transfer media [25-27]. Using γ-Al_2O_3-CuO water-based nanofluid, Bayoumi et al. [28] significantly improved the performance of cooling of an Intel Core i7 CPU, according to experimental and numerical results. The thermal performance of a double pipe heat exchanger with a counter flow mechanism employing Nitrogen-Doped Graphene (NDG) nanofluid was investigated experimentally and numerically by Goodarzi et al. [29-31]. The conclusion from this and similar studies performed was that increasing Reynolds number and nanomaterial loading increases heat transfer rate at a price of pressure drop. Studies are also conducted with micropolar fluids in different channels to understand their effect in linear and micro-rotation velocity[32, 33].

Ajeel et al. [7] studied thermal performance and design parameters in a novel corrugated-curved channel with ZnO/water nanofluid and obtained 2.57 times improvement in thermal hydraulic performance factor. They dealt with various geometric parameters like gap ratio, blockage ratio and pitch angle and tests were carried out at Reynolds number range of 8000-32000. Experiments were performed on Cu/water nanofluid flow and heat transfer in five different serpentine pipes with varied straight section lengths by M. Khoshvaght-Aliabadi et al. [34]. The Performance Evaluation Criterion value of 1.18 is attained by the 0.40 % wt. nanofluid in the serpentine channel with the configuration of low to high straight section lengths. The impact of innovative passive approaches on heat exchanger thermal performance was studied numerically by Feizabadi et al. [35] where varied lengths, twisted pitches, and serpentine pitches of Al_2O_3/water nanofluid was employed in the investigation. The results revealed the impact of altering the straight length and volumetric concentration of nanoparticles on a twisted serpentine tube's thermal performance.

Abed et al. [36] experimentally analyzed the heat transfer and elastic turbulence impact in a serpentine channel with square cross section and obtained up to 200% and 380% increment in

convective heat transfer for low and high polymer concentrated solutions respectively. However, they encountered about 3.3 times more pressure drop to achieve this increment.

Ajeel et al. [37, 38] studied convective heat transfer in corrugated channel experimentally and numerically using SiO_2-water nanofluid. They found that in turbulent flow regime, corrugation as well as using nanofluid significantly enhanced heat transfer rate. They also proposed a novel type of trapezoidal corrugation channel which offered outstanding heat transfer enhancement when compared to a straight channel. Huminic et al. [39] demonstrated the significant influence of TiO_2/water and CuO/water nano-fluids on the entropy generation and thermal performance of helical coiled tube of tube heat exchangers by means of numerical approach and obtained that increasing particle loading results in an increase in Nusselt number and a decrease in entropy generation.

Perwez et al. [40] explored the influence of spherical dimpled surfaces and tear-drop in a rectangular channel with Reynolds numbers ranging from $14x10^3$ to $65x10^3$ using numerical and experimental means. Compared to spherical dimples, rectangular channels with teardrop dimpled surfaces increased heat transmission by 17%. The thermo-hydraulic properties of a dimpled surface were investigated in an experimental investigation by Chen et al. [41] utilizing water as a coolant and forced turbulent flow in an annular channel. Heat transmission was increased to 137% from 25% in the investigation when a dimpled surface was used instead of a plain tube. Different types of artificial roughness, such as corrugated surfaces, dimpled surfaces, and helical wired coils were tested by Garcia et al. [42] in both turbulent and laminar conditions to determine the influence on flow. It was found that when Reynolds Number exceeds 2000, the dimpled surfaces outperform other examined roughness in terms of thermal performance. Bhattad and Sarkar [43, 44] experimentally studied the thermal performance and exergy analysis of a plate heat exchanger using graphene - Al_2O_3 hybrid nanofluid. They obtained 25.36% enhancement in HTC as compared to the base fluid with 0.01% vol. concentration and with a particle volume ratio of 4:1. Al_2O_3-CuO/water hybrid nano-fluid was tested by Selvakumar et al. [45] in electronic heat sinks keeping the volumetric flow rate constant with deionized water to determine its performance. The authors found a 24.35% increment in heat transfer efficiency when using a hybrid nano-fluid with a 0.1% volumetric concentration. They also found that pumping power has to be increased by 12.61% to achieve an improvement of 11.74%. However, an evaluation of thermal efficiency was missing in their work which determines the credibility of the hybrid nano-fluid as a coolant. Bhattad et al. used various hybrid nanofluids with different concentrations in plate heat exchanger and obtained significant improvement in thermal performance. In their studies they used brine based hybrid

nanofluids [46, 47], Al_2O_3–MWCNT [48], Al_2O_3–MgO[49]. All of which resulted in significant heat transfer enhancement, reduction of pumping power requirement and lowering of heat transfer area.

The variation of thermal conductivity in an anulus is studied by Parvin et al. [50] using Al_2O_3/Water nanofluid. They found that heat transfer enhancement occurs as the nanofluid concentration and the Prandtl number is raised. Sundar et al. [51] developed Al_2O_3-Cu nano-composite-based nano-fluids and obtained a 13.56% increase in heat transfer at Re 1750. The study showed the acceptance of the hybrid nano-fluid providing remarks on the thermal efficiency. However, the investigation was limited to the laminar flow regime. Hence, a detailed investigation is required to understand the behavior of Al_2O_3-Cu /water in a turbulent flow regime.

Chapter 3: Working Fluid and Geometry

3.1. Thermophysical Properties of Hybrid Nanofluids

Although nanofluid is originally a two-phase mixture because of the presence of solid particles in the base fluid; still, the physics of conventional two-phase flow may not apply to nanofluid [56]. As nanofluids are composed of nanosized particles and also are of very low concentration, they behave like a fluid rather than a combination of the base fluid and nanoparticles (solid-fluid phase) [57]. Xuan and Roetzel [58] came up with a homogeneous model where the convective heat transport theory equations for fluids were extended to nanofluids. This shows the fact that if the characteristics of base fluids are changed to those of nanofluids, the traditional Nusselt number correlations would be suitable for usage in nanofluids for lower volume concentrations. Nevertheless, many more studies were conducted considering the nanoparticle mixture as a homogenous mixture and the flow approach as a single-phase, and the results obtained are aligned with the results of experimental studies with precision [59, 60]. On the other hand various studies are also done using two phase method [61, 62]. However, using Al_2O_3/water as a working fluid the two-phase Mixture Model was shown to be less accurate in predicting the nano-fluid thermo-hydraulic behavior [63-65]. A maximum disparity of 5.9% was discovered between the Discrete Phase Model and single-phase approaches in this investigation. Since the experimental findings correspond well with the numerical assumptions of the different investigations [66-69], the study proposed adopting a single-phase technique with temperature-independent thermo-physical characteristics for nano-fluids with less than 1.5% volume fraction, provided the best feasible precision in thermo-physical properties is attained for nano-fluids. Table 1 exhibits the thermo-physical properties of the coolants used in the study.

Table 1: Thermo-physical properties of working fluids at T= 303K; reproduced from Saghir et al. [55]

Fluid Name	**Density** (kg/m^3)	**Viscosity** (Pa.s)	**Thermal Conductivity** ($Wm^{-1}K^{-1}$)	**Heat Capacity** (J/kg.K)
Water	995.7	0.0008015	0.614	4174
0.1%vol. Al_2O_3-Cu	1001.3	0.00097	0.6201	4176.83
0.33%vol. Al_2O_3-Cu	1006.64	0.0011	0.6312	4143.5184

0.75%vol. Al_2O_3-Cu	1017.37	0.00139	0.6491	4095.5
1% vol. Al_2O_3-Cu	1023.75	0.0016	0.65727	4067.415

3.2. Computational Geometry

The flow channel which is used in the investigation of the present study is a serpentine channel with a uniform rectangular cross-section. It has three turns with a mean radius of 42.5, 57.5, and 42.5 respectively. The mean length of the channel is taken to be 2577.68mm and the width and the height of the channel cross-section are 15mm and 50mm respectively. Hydraulic diameter (D_h) is measured to be 23.07mm and it is considered constant throughout the channel. The diameter (d) of the hemispherical dimple on the uniform channel is 8mm and thus has a depth of 4mm. The dimples were set in a parallel arrangement with a spanwise (y/d) distance of 3.125 and streamwise distance (x/d) of 11.25 at a stretch up to each curve of the serpentine channel along only one side of its surface. The investigated study's geometrical configuration is evinced in **Error! Not a valid bookmark self-reference.**.

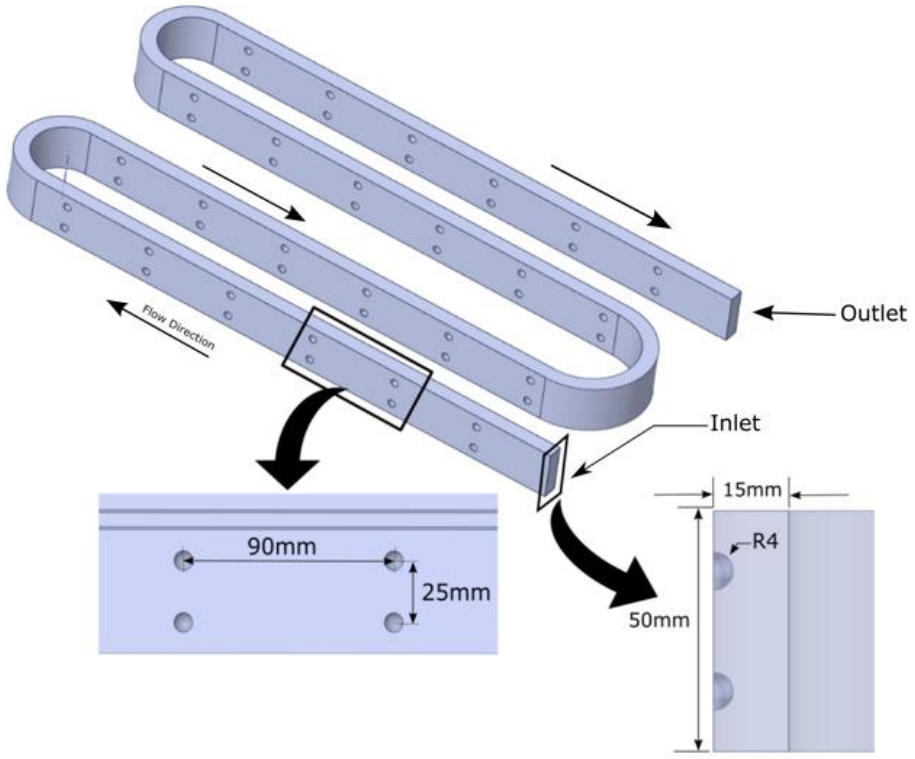

Figure 1: Geometrical configuration of the computational domain

3.3. Grid Sensitivity Analysis

The precision of numerical simulation is dependent on how the grid is made for the fluid domain. The numerical calculations are performed using FVM by ANSYS Fluent. In FVM, the generation of grids across the geometry is crucial for the solution convergence. Tetrahedral meshes were constructed over the serpentine channel with dimple with standard wall treatment. Near the wall, boundary layers were developed to accurately obtain the flow separations and thermal gradient. 13 inflation layers were added to obtain precise results near the wall surface as shown in Figure 2 (a). Again, the element size and the number of nodes have a significant role in predicting the numerical outcomes. Hence, the assessment of optimized mesh using the mesh independence test is required. By varying element size in accordance with the meshes' degree of refinement, the fluctuation of Nu was recorded. Figure 2 (b) demonstrates the variation of Nu with element size. The varies significantly when the element size is 0.18 and 0.16. The value of Nu begins to become stable from element size 0.12mm and remains almost steady for 0.1mm and 0.08mm. Since the magnitude of Nu does not vary considerably with decreasing element size, the computational domain mesh with 0.1 mm element size was chosen for the study. Mesh Refinement Ratio (MRR) is the ratio between the fluid domain's initial cell size and the final cell size, which is used to determine the increase in the node number and element size. Several MRR were examined to comprehend grid independence, and Figure 2 (b) also illustrates the change in averaged Nusselt number with respect to MRR. As the MRR value is increased the change in averaged Nusselt number gradually decreased and became stabilized. Figure 2 (b) reveals that the MRR value of 0.5 provides the best estimation of Nu_{avg} with an error of only 0.09%. The chosen mesh model is represented in Figure 2 (a) and selected for simulations of this study. In total there are 20,23,416 nodes and 45,92,864 elements in the selected mesh model.

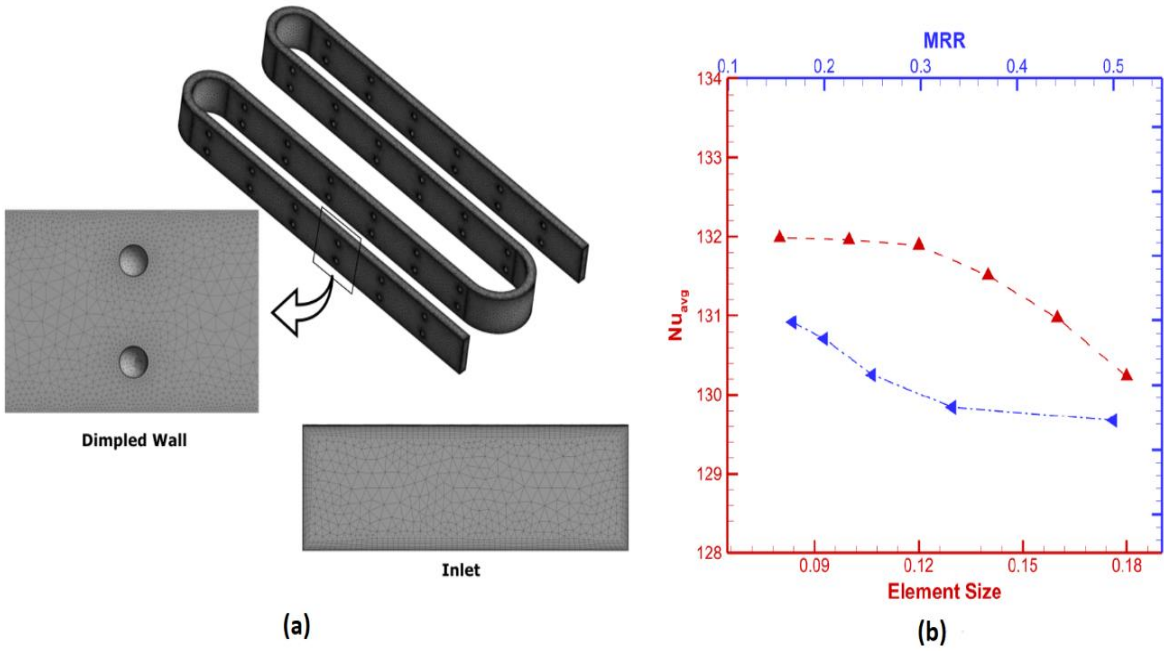

Figure 2: (a) Grid Used (b) Sensitivity Analysis- MRR variation plot

Chapter 4: Computational Methodology

4.1. Numerical Assumptions

The following numerical assumptions are made while performing the numerical study.

1) During the numerical investigations, the working fluid is assumed to be a Newtonian fluid and consequently, the stress to strain ratio is considered constant.
2) As the coolants are considered as Newtonian fluid, the viscosity of the coolants is assumed to be shear rate independent [70].
3) The working thermo-fluids are considered to be incompressible fluids.
4) The combination of nanoparticles and base fluid is regarded to be a homogenous mixture since the particles are dispersed uniformly throughout the liquid [71, 72]. So, the solid nanoparticle's velocity was considered to be the same as the velocity of the base fluid.
5) Numerical simulations were carried out on the assumption of a steady state condition.

The simulations are run in a turbulent flow regime with four different Re in gradually increasing order from $5x10^3$ to $20x10^3$. To solve the 3D Navier-Stokes equation Finite Volume Method was used.

4.2. Governing Equation

Continuity Equation:

$$\frac{\partial}{\partial x_i}(\rho v_i) = 0 \tag{1}$$

Momentum Equation:

$$\rho F_i - \frac{\partial p}{\partial x_i} + \mu\left(\frac{\partial^2 v_i}{\partial x_i^2} + \frac{\partial^2 v_i}{\partial x_j^2} + \frac{\partial^2 v_i}{\partial x_w^2}\right) = \rho\frac{dv_i}{d\tau} \tag{2}$$

$$\rho F_j - \frac{\partial p}{\partial x_j} + \mu\left(\frac{\partial^2 v_j}{\partial x_i^2} + \frac{\partial^2 v_j}{\partial x_j^2} + \frac{\partial^2 v_j}{\partial x_w^2}\right) = \rho\frac{dv_j}{d\tau} \tag{3}$$

$$\rho F_w - \frac{\partial p}{\partial x_w} + \mu\left(\frac{\partial^2 v_w}{\partial x_i^2} + \frac{\partial^2 v_w}{\partial x_j^2} + \frac{\partial^2 v_w}{\partial x_w^2}\right) = \rho\frac{dv_w}{d\tau} \tag{4}$$

Energy Equation:

$$\frac{\partial T}{\partial \tau} + v_i \frac{\partial T}{\partial x_i} + v_i \frac{\partial T}{\partial x_j} + v_j \frac{\partial T}{\partial x_k} = \frac{\lambda}{\rho c_p}\left(v_i \frac{\partial^2 T}{\partial x_i^2} + v_i \frac{\partial^2 T}{\partial x_j^2} + v_j \frac{\partial^2 T}{\partial x_k^2} \right) \quad (5)$$

4.3. Turbulence Model Selection

The precision of the complex geometry model's analysis is largely dependent on the selection of a suitable turbulence model. It is important to consider flow physics, as well as the level of precision, which is necessary while selecting a relevant model for a specific problem. Kumar et al. [73] studied the fluctuation of the Nusselt number with Re for several turbulence models with the findings from the Dittus-Boelter equation for a smooth walled channel. They found that the equation results and the results from the RNG k-e model were very close. According to Yadigaroglu et al. [74], in terms of performance, the k-epsilon model was not satisfactory in predicting turbulent flow dynamics in flow regions with narrow widths. In the investigation of the thermal-hydraulic behavior, Rahimi-Esbo et al. [75] developed a new modified model of the SST k–ε. The use of a precise, distinctive model for the analysis of this kind of flow pattern is then demonstrated to have some advantages. Time and memory space is highly prioritized during ANSYS simulation and modeling and a model named Reynolds Stress Equation Model (RSM) turbulence model, needs more time and data with increasing computational accuracy [76]. It uses 15%-20% more memory and around 50% to 60% more time in a single iteration than the k–ε and k–ω turbulence models. Since time and memory space are highly prioritized during ANSYS simulation and modeling, the RSM turbulence model is avoided here for the optimized result. Ahmad et al [77, 78] used the RNG k–ε model to examine the enhancement of heat transfer of turbulent nanofluid forced-flow in a duct introducing a triangular rib. This turbulence model was developed by the use of a rigorous statistical approach known as the renormalization group RNG theory [79]. This theory was obtained from the Navier-Stokes equations by filtering. The Boussinesq hypothesis forms the basis for the RNG k–ε model, which links the Reynolds tensor to the gradient of the mean velocity, turbulent viscosity, and turbulent kinetic energy. When compared to the normal k–ε model, the RNG model's inclusion of refinements results in a significant improvement in the accuracy of the prediction of quickly strained flow. Unlike the Standard k–ε model, the RNG k–ε model also provides better results for a wide range of Reynolds numbers because this theory gives a differential formula that has been analytically derived and it considers low Reynolds number effect too. Because of these benefits, the RNG k–ε model is superior to the Standard k–ε model in terms of accuracy and dependability for a greater variety of flow conditions[80, 81]. Hence,

RNG k–ε model was implemented for numerical simulations of the present study. The model is expressed by the **equations 6 and 7** [82].

For $0.5 < Pr < 120$ and $6.0 \times 10^3 < Re < 1.0 \times 10^7$,

$$\frac{\partial}{\partial t}(\rho k) + \frac{dy}{dx_i}(\rho \epsilon u_i) = \frac{d}{dx_j}\left(a_k \mu_{eff} \frac{dk}{dx_j}\right) + G_k + G_b - \rho\epsilon - Y_M + S_k \quad (6)$$

$$\frac{\partial}{\partial t}(\rho \epsilon) + \frac{dy}{dx_i}(\rho \epsilon u_i) = \frac{d}{dx_j}\left(a_k \mu_{eff} \frac{dk}{dx_j}\right) + C_{1\epsilon}\frac{\epsilon}{k}(G_k + C_{3\epsilon}G_b) - C_{2\epsilon}\rho\frac{\epsilon^2}{k} - R_\epsilon + S_\varepsilon \quad (7)$$

Here, C1ε, and C2ε are developed from the theory as model constants. The values of these constants are taken as 1.44 and 1.92 respectively.

4.4. Boundary Condition:

All the simulations were performed using a steady and uniform heat flux of 50KW/m^2 on all the surfaces of the serpentine channel. Turbulent flow regime was studied with Re ranging from 5x10^3 to 20x10^3 with an interval of 5x10^3. The inlet temperature for water and nanofluid was maintained at T_0 = 303K and the gauge pressure at the outlet was kept at 0 Pa. Implicit solver was selected for solving the governing equations. The application of pressure-velocity coupling was carried out using SIMPLE algorithm, and then normal pressure interpolation was carried out. As the convergence criteria, for continuity and momentum equations, the Root Mean Square (RMS) value was set to 10^6 and for energy, the corresponding value was set to 10^9. ANSYS 2020 R1 was used for performing all the simulations of the study.

Equation 9 was used as the formula for the Reynolds number. Corresponding to the Reynolds number, the velocity of the coolant was calculated using this equation. Here, v is the inlet velocity, ρ is the density of the coolant, υ stands for the viscosity of the coolant and D_h is the hydraulic length of the geometry. The value of D_h is calculated to be 23.07mm from **equation 8**.

$$D_h = \frac{4.a.b}{a+b} \quad (8)$$

Here, a and b are width and height of the rectangular cross section of the channel.

$$Re = \frac{\rho v D_h}{\mu} \quad (9)$$

The heat transfer coefficient was calculated using **equation 10**, where Q̇ represents the constant heat flux, A is the heat transfer area, and T_w is the wall temperature [14].

Equation 10 was used for calculating the fluid's bulk temperature. V_m is the maximum velocity

$$h = \frac{\dot{Q}}{A(T_w - T_{bulk})} \tag{10}$$

along the channel length whereas τ_w represents the shear stress at the wall.

$$T_{bulk}(l) = T_w(l) + \frac{\dot{Q} V_m}{\tau_w C_P} \tag{11}$$

$$h_{avg} = \frac{1}{L}\int_0^L h(l)dl \tag{12}$$

The average heat transfer coefficient of the channel was obtained from **equation 12** where L represents the total length of the flow channel. [14]

The average Nusselt number was calculated using **equation 13**.

$$Nu_{avg} = \frac{h_{avg} D_h}{k_0} \tag{13}$$

The friction factor was calculated using **equation 14** where ΔP_{avg} is the average pressure drop along the length of the channel [10].

$$f = \frac{2\Delta P_{avg} D_h}{4\rho L v^2} \tag{14}$$

4.5. Validation:

For the validation of the study, at first, the smooth serpentine channel was validated by comparing the results with the experimental correlations produced for Nu_{avg} by Karale et al. [83]. They used a serpentine channel made up of 10 units to conduct flow and heat transfer studies. The geometry was replicated and simulation was carried out with the same boundary conditions and specified mesh configurations of the present study and water with inlet temperature 298K was used as the working fluid. Figure 3(a) shows the comparison between the present study and the experimental values obtained by Karale et al. The Figure demonstrates that the numerical findings correspond well with the experimental data within a satisfactory margin of error. Nevertheless, the maximum deviation was 3.52% at Re 613.

Since similar studies incorporating dimples in the serpentine channel are not available and the

authors are studying it for the first time, the validation of the serpentine dimple channel is accomplished also through a rectangular dimpled channel. The authors followed the experimental and numerical study investigated in a rectangular channel by Rao et al. [84]. To determine how different dimple configurations affect heat transmission and frictional flow over dimpled surfaces of varying dimple forms in turbulent flows, they carried out an experimental investigation and a computational analysis in a channel with a rectangular cross-section. Keeping the boundary conditions same and following the specified mesh configurations of the present study and using water as the coolant, the simulation was performed. Figure 3(b) displays the comparability between the Nusselt numbers of the present study with the numerical and experimental Nusselt numbers obtained from Rao et al [84]. A good agreement between the Nusselt number obtained from the present study and the experimental and numerical Nusselt number values are noticed with a reasonable percentage of error. The maximum error obtained was with the experimental value and which is about 11.2% whereas the largest deviation seen for the CFD result was 5.05%. Both of the largest deviations were recorded for Re 18.907 x 10^3.

Upon evaluating the aforementioned comparative studies, it is evident that the numerical results are quite close to the experimental investigation's results, which validate the numerical results presented for the spherical dimpled serpentine channel.

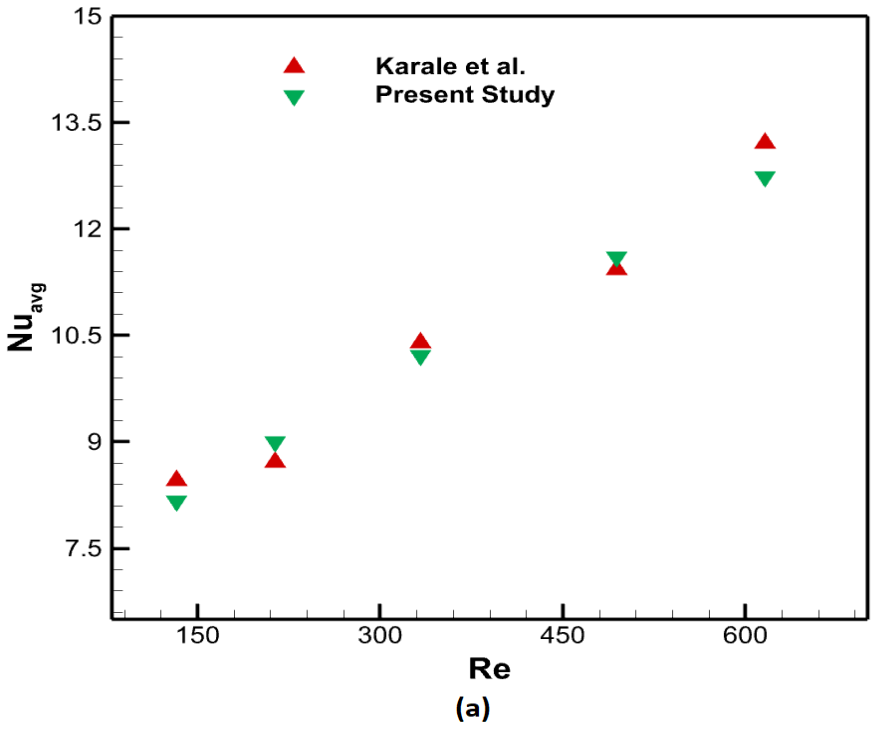

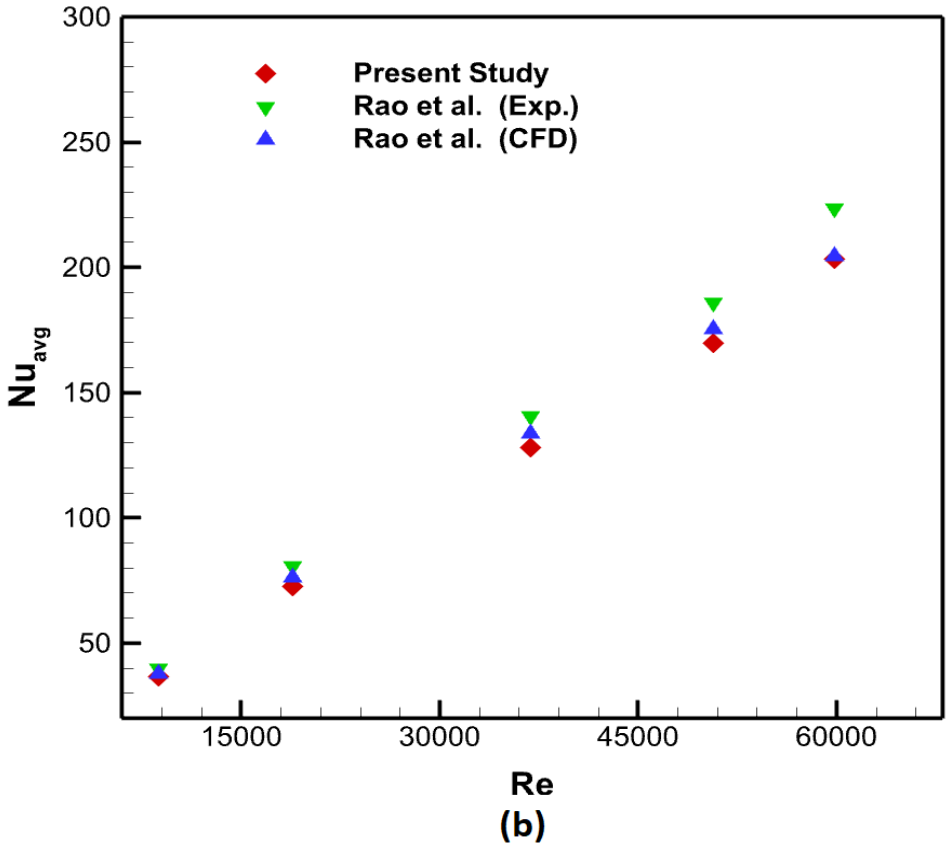

Figure 3: Validation of the present study with (a) Karale et al. [83] for serpentine channel and (b) Rao et al. [84] for dimpled channel

Chapter 5: Results and Discussions

This study compares the heat transfer coefficient, pressure drop, and thermal performance of serpentine smooth and dimple channels. Both local and global parameters were assessed in order to find the optimum result. The study is comprised of two segments. Firstly, the comparison of the thermal efficiency of dimpled serpentine channel and smooth serpentine channel with rectangular cross-section was assessed. Secondly, investigations and comparisons of the thermal performances of the better channel with hybrid nanofluid of Al_2O_3-Cu with water as base fluid is considered to find the best combination of passive heat transfer enhancement among the studied cases. Here, Al_2O_3-Cu nanofluid with φ = 0.1%, 0.33%, 0.75% and 1% volume fraction were studied in a dimpled channel considering single-phase approach. Turbulent flow in the channel was studied with varied Reynolds numbers from $5x10^3$ to $20x10^3$ with an interval of $5x10^3$.

5.1. Performance Evaluation of Serpentine Channel with Spherical Dimple Using Water as Coolant:

5.1.1. Heat Transfer Coefficient (h_{avg})

Figure 4: Comparison between the smooth and the dimpled channel with water as coolant (a) Heat transfer coefficient, (b) Pressure drop, (c) PEC

Figure 5: Velocity distribution contour; (A) At various position of the channel, (B) Variation of flow velocity for different channels and nanofluid concentrationsFigure 4 (a) shows the average HTC with respect to Re for a smooth and dimpled serpentine channel. From the graph, it is evident that the heat transfer coefficient goes up as dimples are added to the computational domain. There are 12 dimples on one side of each turn making a total of 48 dimples in the test section. The dimples are arranged uniformly in a parallel arrangement with a spanwise (y/d) distance of 3.125 and a streamwise distance (x/d) is 11.25. The dimpled surface creates obstructions for fluids to flow, which increases the turbulence and makes heat transfer go up. Also, the dimpled s face impacts the physical properties of the coolant because of the turbulence around dimple vicinities over a fluid pattern. As heat transmission is a surface phenomenon, the changes in the surface caused by dimple shapes aid in increasing the heat transfer as shown in Figure 4: Comparison between the smooth and the dimpled channel with water as coolant (a) Heat transfer coefficient, (b) Pressure drop, (c) PEC

Figure 5: Velocity distribution contour; (A) At various position of the channel, (B) Variation of flow velocity for different channels and nanofluid concentrationsFigure 4 (a). Moreover, **Error! Reference source not found.** clearly indicates that the temperature in the dimple wakes and at flow reattachments is lower than in other areas, whereas the temperatures in separation zones are higher. It signifies that the reattachment and the vortices produced from dimples generate a significant heat transfer zone. The boundary layer separation causes a low heat transmission zone. A stronger heat transfer occurs in the upstream region of protrusions due to the flow impinging on the protrusion's front. However, when separation occurs, heat transmission decreases.

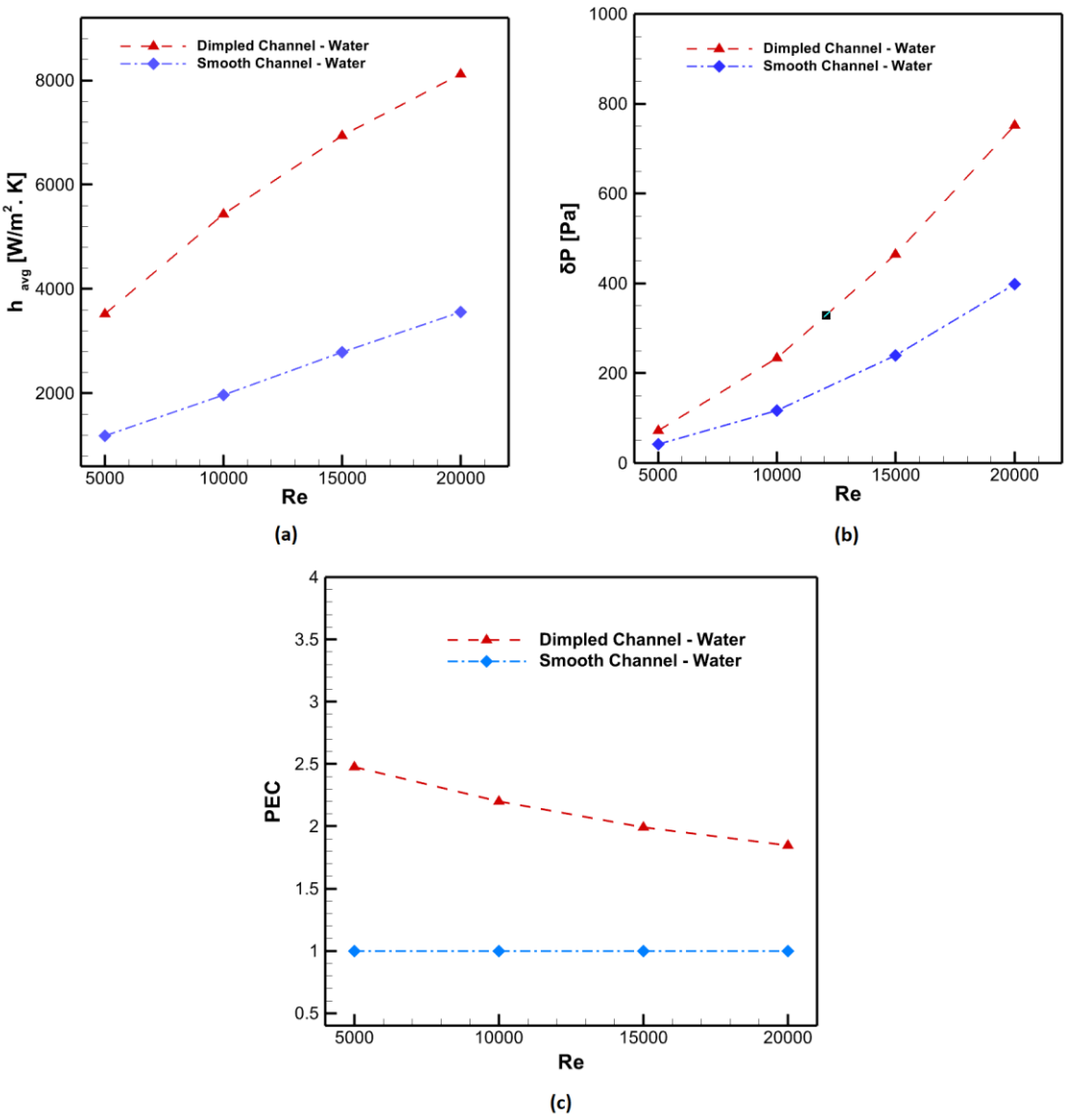

Figure 4: Comparison between the smooth and the dimpled channel with water as coolant (a) Heat transfer coefficient, (b) Pressure drop, (c) PEC

5.1.2. Pressure Drop and Friction Factor:

The investigation also compared the pressure losses and friction factors of the smooth and dimpled serpentine channels. There was a greater pressure drop and friction coefficient in the dimpled serpentine channel than in the smooth channel. Due to the obstructive nature of dimpled surfaces, the impact causes a rise in both the pressure drop and the friction coefficient. Velocity was decreased because of the obstructions caused by dimples, especially in the wake regions of the dimples. Figure 4: Comparison between the smooth and the dimpled channel with water as coolant (a) Heat transfer coefficient, (b) Pressure drop, (c) PEC

Figure 5: Velocity distribution contour; (A) At various position of the channel, (B) Variation of flow velocity for different channels and nanofluid concentrationsFigure 4 (b) shows the pressure drop with respect to Re. Among the analyzed cases, the lowest average pressure drop was noticed for Re 5 $x10^3$ and the maximum pressure drop was recorded for Re $20x10^3$ for both cases. For Re 5 $x10^3$, the average pressure drop recorded for the smooth serpentine channel was 42.18 Pa whereas, for the dimpled serpentine channel, it was 71.69 Pa and for Re 20 $x10^3$, on average, about 397.71 Pa and 752.39 Pa.

5.1.3. Performance Evaluation Criterion (PEC_{rs}):

The Performance Evaluation Criterion (PEC) for the smooth serpentine channel and the dimpled serpentine channel were investigated using **Equation 14**. It evaluates the thermal performance by taking not only heat transfer enhancement but also pressure drop into account [85]. Figure 4: Comparison between the smooth and the dimpled channel with water as coolant (a) Heat transfer coefficient, (b) Pressure drop, (c) PEC

Figure 5: Velocity distribution contour; (A) At various position of the channel, (B) Variation of flow velocity for different channels and nanofluid concentrationsFigure 4 (c) shows the PEC values for both types of channels. Since here PEC is calculated with respect to the smooth serpentine channel with water as a coolant by the aforementioned formula, any value above 1

is considered to have better thermal performance. For dimpled serpentine channel the PEC values obtained for Reynolds number $5x10^3$, $10x10^3$, $15x10^3$ and $20x10^3$ were 2.47, 2.20, 1.99 and 1.84 respectively. These values indicate significantly better thermal efficiency for the dimpled serpentine channel as compared to the smooth channel.

$$PEC_{rs} = \frac{{Nu_{rs}}/{Nu_{ss}}}{\left({f_{rs}}/{f_{ss}}\right)^{1/3}} \quad (15)$$

5.2. Performance Evaluation of Dimpled Serpentine Channel Using Al_2O_3-Cu Nanofluid:

Since the comparative study between the serpentine channel with smooth surface and dimpled surface concludes that the dimpled serpentine channel provides better thermal performance, for further heat transfer enhancement in passive technique, studies were conducted with the better performing channel using Al_2O_3-Cu hybrid nanofluid as the working fluid. For getting an overall comparison, investigations were carried out in the same Re numbers as before.

5.2.1. Analysis of Velocity Distribution:

Figure 5: Velocity distribution contour; (A) At various position of the channel, (B) Variation of flow velocity for different channels and nanofluid concentrations (A) shows the velocity distribution for water in the dimpled channel at Re 20 $x10^3$ and Figure 5: Velocity distribution contour; (A) At various position of the channel, (B) Variation of flow velocity for different channels and nanofluid concentrations (B) shows the velocity distribution using nanofluid of 0.1%, 0.33%, 0.75%, and 1% volume fractions of Al_2O_3-Cu at Re 20 $x10^3$. From the figure it can be seen that maximum velocity was for 1% vol. Al_2O_3-Cu followed by 0.75%, 0.33%, and 0.1% respectively and the lowest was observed for water in the smooth channel. Because of dimple protrusions, near the dimpled surfaces, secondary flow is induced. Since there are two dimples along the width of the channel there are two prominent regions of secondary flow, aligned with the dimples. The fluid velocity near the dimples is higher and it can be explained by Bernoulli's principle. According to Bernoulli's principle, if the cross-sectional area decreases, the fluid velocity should increase to maintain continuity. Besides this, velocity close to the periphery is lower because of the boundary layer's effect. For the dimpled channel, albeit the velocity profiles for water and the nanofluids are alike qualitatively, however

quantitatively, the velocity magnitudes of φ = 0.1%, 0.33%, 0.75%, and 1% nanofluid are not the same. The main reason for this variation is the difference in viscous forces and buoyancy. Moreover, more density and viscosity make the dynamic and thermal boundary layer for nanofluid thicker as compared to the base fluid water. As the inclusion of Al_2O_3-Cu nanoparticle is done to water for preparing the nanofluid, it makes the intermixing of the fluid layers better, consequently intensifying the induced secondary flow. This phenomenon leads to the conclusion that the more the incorporation of nanoparticles, the greater the velocity magnitude.

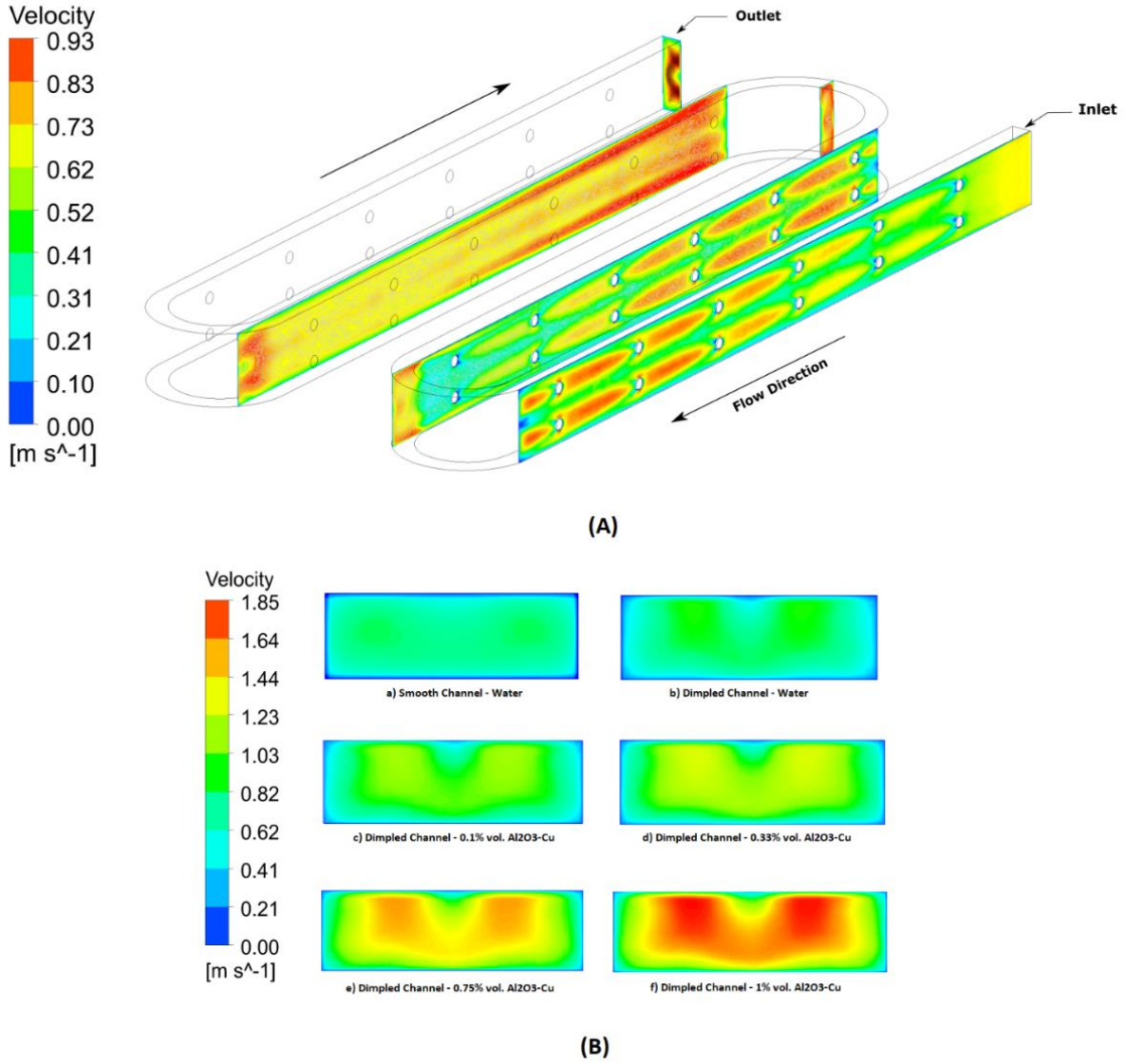

Figure 7: Velocity distribution contour; (A) At various position of the channel, (B) Variation of flow velocity for different channels and nanofluid concentrations

5.2.2. Temperature Distribution Analysis:

Error! Reference source not found. depicts the temperature changes along the smooth channel walls and the dimpled channel while using water and different concentrations of Al_2O_3-Cu nanofluid as coolant at Re $15x10^3$. The **Error! Reference source not found.** shows the temperature contour taken at a distance of distance 0.285m in the xy plane. It is observed that

for the dimpled channel, as the concentrations of the nanofluid increases, thermo-physical characteristics of the working fluid get better. Consequently, the temperature of the wall of the channel decreases. The wall temperature obtained for 0.1 % vol. nanofluid is lower than for water, followed by 0.33% vol. and 0.75% vol. respectively, and the lowest temperature is obtained for 1 vol. % nanofluid. As seen in the figure, the temperature of the wall of the channel with dimples was much lower than that of the channel without dimples. The lowest temperature was obtained in the dimpled channel with 1% vol. concentration is 309.90K at the surrounding areas of the dimples. The dimpled surface played a big part in lowering the temperature of the walls by causing secondary flow close to the dimples. In addition, dimpled surfaces hamper the boundary layer growth, which causes the intensity of the turbulent flow to rise. Increased Turbulent Intensity (TI) mostly made heat transfer better, which caused the wall temperature to drop. Nanofluids usage in the dimpled serpentine channel further improved the thermal performance of the heat exchanger. As a result, the temperature at the wall is reduced more as the nanofluid concentration is increased.

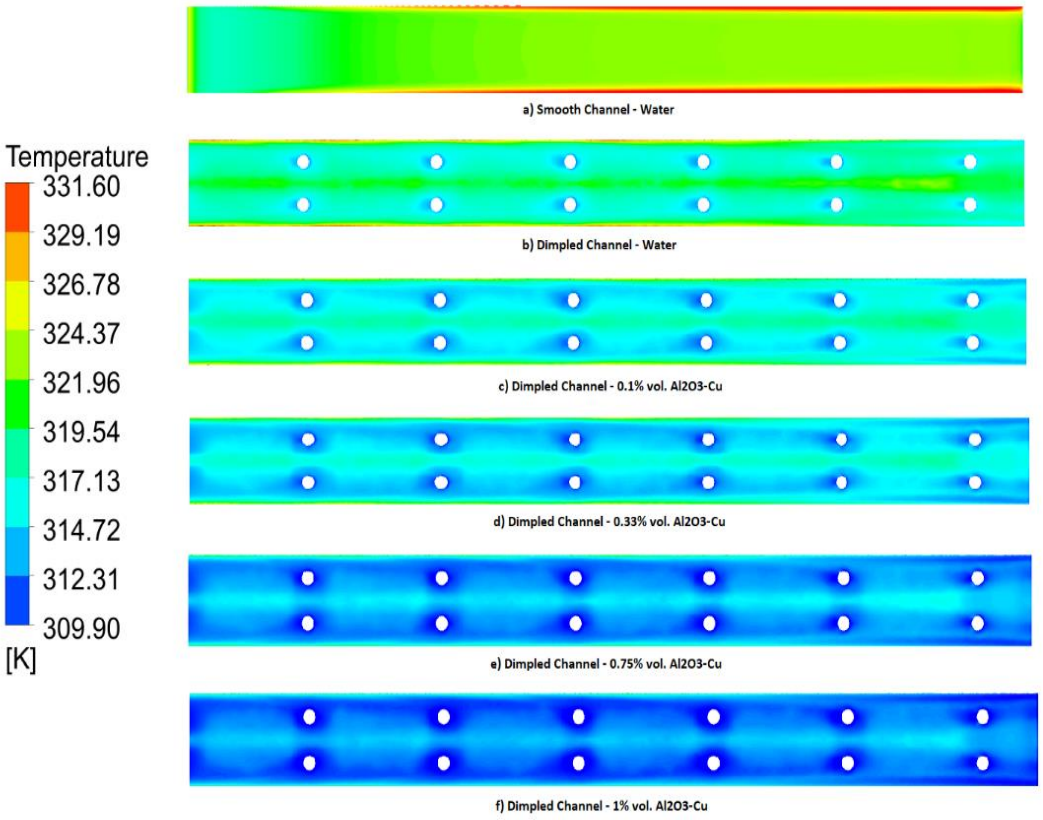

Figure 8: Variation of temperature for different channels and nanofluid concentrations

5.2.3. Turbulence Intensity:

Turbulence Intensity (TI) is a key factor in improving heat transfer. So, the higher the value of TI, the higher the value of the heat transfer coefficient would become. Figure 7: Variation of turbulence intensity for different channels and nanofluid concentrations shows the change in TI for the plain serpentine channel and dimpled serpentine channel with the base fluid water and then also with Al_2O_3-Cu/water nanofluid with φ = 0.1%, 0.33%, 0.75%, and 1% at the dimple closest to the outlet (80 mm from the outlet) for the value of 20 $x10^3$ Re. The value of turbulence intensity is found to be higher in the channel with dimpled walls than in a smooth channel, as the dimple jaggedness are significant for making more turbulence near the walls. Figure 7: Variation of turbulence intensity for different channels and nanofluid concentrations shows that the value of TI is maximum for 1% volume Al_2O_3-Cu, then 0.75% vol., 0.33% vol. followed by 0.1% volume, and then the base fluid. TI is recorded lowest for the base fluid. It can be said that the characteristics of turbulence have the greatest impact on the presence of nanoparticles. So, when the volume fraction of nanofluid goes up, the value of TI is also increased. Also, the figure shows that the value of TI is highest near the dimples and walls of each case and it decreases gradually away from the walls of the flow regime. The value of TI is lowest in the center of the fluid domain. Hence, it is quite evident that the introduction of dimpled protrusions readily increased the turbulence intensity and nanofluids corresponding to their concentration increased the TI even more.

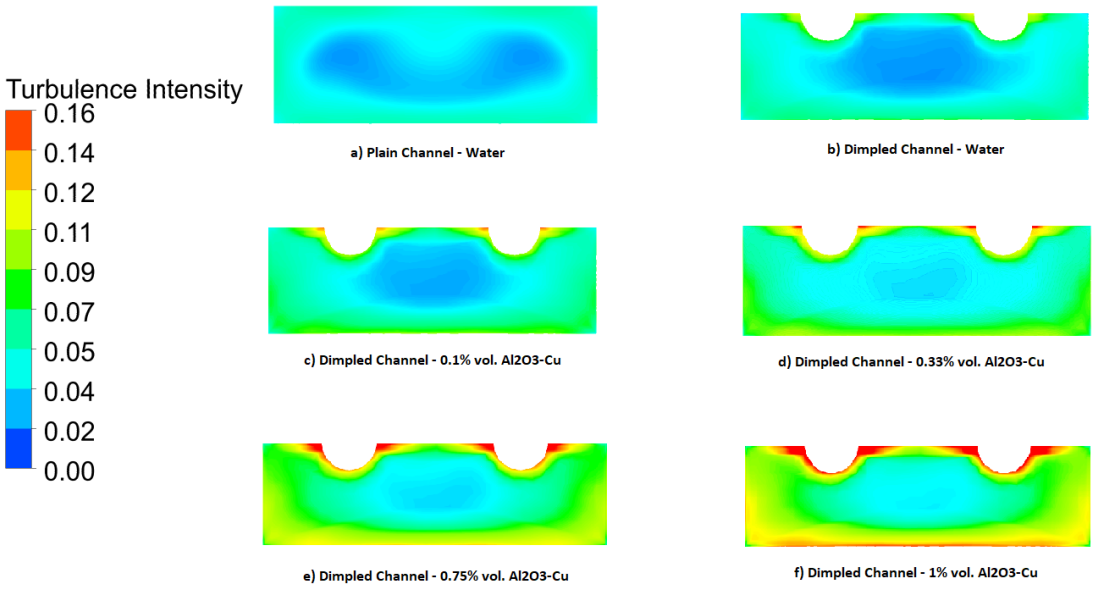

Figure 9: Variation of turbulence intensity for different channels and nanofluid concentrations

5.2.4. Heat Transfer Enhancement:

In Figure 8: Comparison of water and various concentrations of Al_2O_3-Cu nanofluid Average Heat Transfer Coefficient (HTC) and Re are plotted along the y and x axis to obtain the graphic comparison between the working fluids of this study by showing the variation of HTC as a function of Re. HTC was calculated using **equations 9 and 11**. From the figure, it is clear that 1% vol. Al_2O_3-Cu nanofluid has the highest HTC as compared to other fluids. In the dimpled serpentine channel, the rate of heat transfer increased gradually with the increasing volume concentration of the nanofluid. With respect to water, HTC increased 58.15% for Re $5x10^3$, and for Re $20x10^3$, about 226% increment has been recorded. Since the thermophysical characteristics like thermal conductivity, viscosity, etc. of the coolants were enhanced when nanoparticles with greater thermal conductivities were added to the base fluid, the improvement in heat transfer could be seen. As a consequence of the enhanced thermal conductivity, nanofluids are capable of enhancing the coefficient of heat transfer. Moreover, the same fluid has a better heat transfer rate for higher Re. For 1% Al_2O_3-Cu, the heat transfer rate almost doubled from 5.57 $kW/m^2.K$ to 11.51 kW/m^2. K for Re 5 $x10^3$ to Re 20 $x10^3$. Fluid flow with a higher Re-experiences more turbulence than that of lower Re flows which ensures significant mixing of the boundary layer and the bulk fluid. This eventually increases the heat transfer rate.

However, the rate of increase of HTC with Re gradually decreases with the increment of Re.

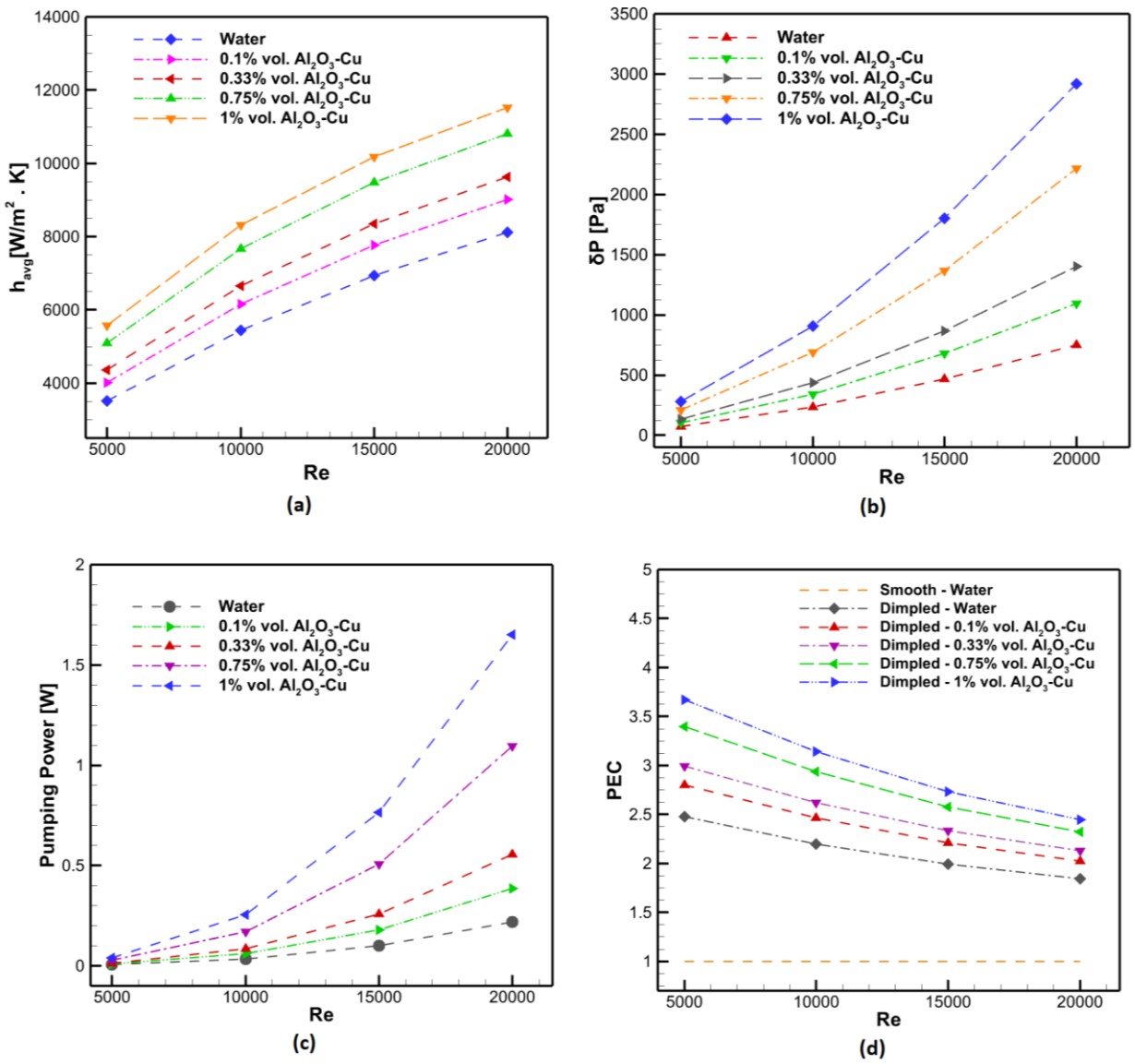

Figure 10: Comparison of water and various concentrations of Al_2O_3-Cu nanofluid

5.2.5. Pressure Drop:

The addition of nanoparticles increases the coolant's thermal conductivity, as explained before. Nonetheless, the addition of nanoparticles increases viscosity and density, leading to pressure drop increment.

Figure 8: Comparison of water and various concentrations of Al_2O_3-Cu nanofluid (b) illustrates the average pressure decrease for each of the analyzed scenarios when Re is varied. Compared to a smooth serpentine channel, a dimpled serpentine channel exhibits a greater pressure drop

owing to the obstructions caused by dimpled protrusions on the surfaces of the fluid's motion. In addition, the figure demonstrates that the addition of nanoparticles raised the average pressure drop. Because of the increased cohesions among nanoparticles, as the weight concentration rises, the average pressure drops increase gradually. Therefore, 1% vol. Al_2O_3-Cu nanofluid exhibited the maximum pressure loss, which gradually reduced and reached its minimum value for the base fluid. Furthermore, as can be seen in Figure 8: Comparison of water and various concentrations of Al_2O_3-Cu nanofluid (b), for a particular nanofluid the pressure drop rises as Re increases. Since the rise in Re causes an increase in the hydrodynamic entry length, the velocity gradient and shear stress at the entrance length's wall area increase. Consequently, the pressure drops increase in the entry area, which causes the average pressure drop to rise as Re increases.

$$\text{Pumping Power} = \frac{\pi}{4}.D_h.v.\ \Delta P \qquad (16)$$

Equation 15 was used to calculate the pumping power [10]. The pumping power is shown in Figure 8: Comparison of water and various concentrations of Al_2O_3-Cu nanofluid (c) as a function of Re. The nanofluid containing 1% Al_2O_3-Cu has the maximum pumping power, which falls with decreasing weight concentrations, while the smooth channel has the lowest pumping power among all.

5.2.6. Performance Evaluation Criterion (PEC_{nf}):

As discussed, pressure drop and heat transfer are both higher in the dimpled serpentine channel than in the smooth serpentine channel. Since pressure drop is intrinsically tied to pumping power and the effectiveness of cost, as the pressure drop goes up, the amount of pumping power needed goes up as well. So, to figure out how well the geometry works, the thermal efficiency of the dimpled surface was measured using the Performance Evaluation Criterion (PEC), which is shown in **Equation 16** [73, 85]. For thermal efficiency, PEC looks at both the case where heat transfer improves and the case where the pressure drops. Also, just like with a rough-surfaced dimpled channel, adding nanoparticles to the base fluid water, increases the heat transfer at a cost of a drop in pressure. In order to put the nanofluid to use, the conclusion needs to take not only the rise in heat transfer but also the decrease in pressure into consideration. Using the Performance Evaluation Criterion or Thermal Performance Factor (TPF) for nanofluids [78, 86, 87], the thermal performance of nanofluids was measured using **Equation 16**.

$$PEC_{nf} = \frac{Nu_{nf}/Nu_{bf}}{\left(f_{nf}/f_{bf}\right)^{1/3}} \quad (17)$$

If the PEC value is higher than 1, it is clear that improvement in heat transfer is more than pressure loss. If, on the other hand, the PEC value is lower than 1, it means that pressure loss is greater than heat transfer improvement. The thermal performance for all the cases studied with different Reynolds numbers is shown in Figure 8: Comparison of water and various concentrations of Al_2O_3-Cu nanofluid (d). As seen in the figure, the PEC values for each case of a dimpled channel are all higher than 1. In addition to that, it is also evident from the figure that based on thermos-hydraulic performance, a heat exchanger with a dimpled serpentine channel would be better than one with a smooth serpentine channel. When compared to the smooth serpentine channel, the maximum PEC value of 1.47 for the dimpled channel was reached at Re 5 x 10^3, which is This was achieved by utilizing water as the coolant. It was observed that as Re went up, the value of PEC went down, and the minimum improvement in thermal performance was found to be 84.51% at Re 20 x10^3. With higher volume concentrations, the thermal efficiency of Al_2O_3-Cu/water nanofluid in the dimpled serpentine channel got better. Consequently, 1% Al_2O_3-Cu nanofluid had the best thermal performance, followed by 0.75%, 0.33%, and base fluid, which had the worst performance. For φ = 1% Al_2O_3-Cu, the thermal performance went up by a maximum of 267.04%, which is an outstanding improvement in terms of the distinctiveness of the investigations done. It was noted that the maximum increase in thermal performance was 239.67%, 199.18%, and 179.93% for φ = 0.75%, 0.33%, and 0.1% Al_2O_3-Cu nanofluid, respectively at Re 5 x10^3. This is a remarkable as well as recognizable improvement in thermal performance for industrial applications.

From the discussion, it is clear that as Re went up, the value of PEC went down, and for all of the cases that were investigated, Re 5 x 10^3 was the highest value of PEC found. So, the discussion leads to the conclusion that a dimpled serpentine channel with base fluid water and nanofluids of different concentrations will work better at lower ranges of Re in a turbulent flow regime.

Chapter 6: Conclusion

6.1. Conclusion

This study investigates the thermos-hydraulic performance of a serpentine channel with three steps passive heat transfer enhancement technique. A serpentine channel surface is modified by introducing dimples and Al_2O_3-Cu/water hybrid nanofluid is used as the working fluid for obtaining better thermal efficiency in turbulent flow regimes. The following conclusions are reached while performing this study.

- At first, using only the base fluid water, with respect to the smooth serpentine channel, for the dimpled channel, about 147.62% increment in thermal efficiency is obtained at Re $5x10^3$. This is the highest improvement for the base fluid among the test cases for four different Reynolds numbers. As the Re increases, the improvement in PEC gradually decreases. 120.01%, 99.29%, and 84.51% increment in performance are obtained for Re 10 $x10^3$, 15 $x10^3$ and 20 $x10^3$ respectively.
- Further investigations of the dimpled serpentine channel with four different concentrations of Al_2O_3-Cu/water hybrid nanofluid reveal that the heat transfer performance is improved by 267.04%, 239.67%, 199.18%, and 179.93% for φ = 1%, 0.75%, 0.33% and 0.1% volume concentrations respectively at Re $5x10^3$. For nanofluid working medium too, the rate of thermal performance enhancement reduces with an increase in Re. However, the values of PEC which are obtained in the study after modifications and changing heat transfer medium fluid are extraordinary.
- The heat transfer performance improves at a pressure drop cost; thus, higher pumping power is required.

So, the investigation findings suggest that 1% vol. Al_2O_3-Cu/water hybrid nanofluid with the dimpled surfaced serpentine channel will provide the best performance in terms of heat transfer enhancement among all the test cases. For lower Re, the comparative improvement is more as compared to higher Re.

6.2. Recommendation for future works

To explore the thermal and hydraulic performance of nanofluids as a coolant, only a computational investigation of single-phase flow is conducted due to a lack of experimental equipment. However, the following recommendations are provided for further works:

- MHD effect can be analyzed in this channel using the same or different nanofluids.

- Similar study can be done using different nanofluids and different boundary conditons.
- Different shapes of Jaggedness can be implemented in the smooth channel and a parametric comparison study can be done.
- Introducing turbulators and Ribs in the serpentine channel can a scope for further research.

References

1. Raza, J., F. Mebarek-Oudina, and A.J. Chamkha, *Magnetohydrodynamic flow of molybdenum disulfide nanofluid in a channel with shape effects.* Multidiscipline Modeling in Materials and Structures, 2019.
2. Selimefendigil, F., H.F. Öztop, and A.J. Chamkha, *Role of magnetic field on forced convection of nanofluid in a branching channel.* International Journal of Numerical Methods for Heat & Fluid Flow, 2019.
3. Chamkha, A.J., *On laminar hydromagnetic mixed convection flow in a vertical channel with symmetric and asymmetric wall heating conditions.* International Journal of Heat and Mass Transfer, 2002. **45**(12): p. 2509-2525.
4. Alzahrani, S. and S. Usman, *CFD simulations of the effect of in-tube twisted tape design on heat transfer and pressure drop in natural circulation.* Thermal Science and Engineering Progress, 2019. **11**: p. 325-333.
5. Nalavade, S.P., C.L. Prabhune, and N.K. Sane, *Effect of novel flow divider type turbulators on fluid flow and heat transfer.* Thermal Science and Engineering Progress, 2019. **9**: p. 322-331.
6. Bhattad, A., J. Sarkar, and P. Ghosh, *Hydrothermal performance of different alumina hybrid nanofluid types in plate heat exchanger.* Journal of Thermal Analysis and Calorimetry, 2020. **139**(6): p. 3777-3787.
7. Ajeel, R.K., K. Sopian, and R. Zulkifli, *A novel curved-corrugated channel model: Thermal-hydraulic performance and design parameters with nanofluid.* International Communications in Heat and Mass Transfer, 2021. **120**: p. 105037.
8. Ajeel, R.K., K. Sopian, and R. Zulkifli, *Thermal-hydraulic performance and design parameters in a curved-corrugated channel with L-shaped baffles and nanofluid.* Journal of Energy Storage, 2021. **34**: p. 101996.
9. Ajeel, R.K., et al., *Numerical investigation of binary hybrid nanofluid in new configurations for curved-corrugated channel by thermal-hydraulic performance method.* Powder Technology, 2021. **385**: p. 144-159.
10. Ahmed, F., et al., *Assessment of thermo-hydraulic performance of MXene-based nanofluid as coolant in a dimpled channel: a numerical approach.* Journal of Thermal Analysis and Calorimetry, 2022. **147**(22): p. 12669-12692.
11. Keimanesh, M., et al., *Study of a third grade non-Newtonian fluid flow between two*

parallel plates using the multi-step differential transform method. Computers & Mathematics with Applications, 2011. **62**(8): p. 2871-2891.

12. Ajeel, R.K., et al., *Assessment and analysis of binary hybrid nanofluid impact on new configurations for curved-corrugated channel.* Advanced Powder Technology, 2021. **32**(10): p. 3869-3884.
13. Ajeel, R.K., W.-I. Salim, and K. Hasnan, *Design characteristics of symmetrical semicircle-corrugated channel on heat transfer enhancement with nanofluid.* International Journal of Mechanical Sciences, 2019. **151**: p. 236-250.
14. Ahmed, F., et al., *The impact of D-shaped jaggedness on heat transfer enhancement technique using Al2O3 based nanoparticles.* International Journal of Thermofluids, 2021. **10**: p. 100069.
15. Ahmed, F., et al., *Numerical investigation of the thermo-hydraulic performance of water-based nanofluids in a dimpled channel flow using Al2O3, CuO, and hybrid Al2O3–CuO as nanoparticles.* Heat Transfer, 2021. **50**(5): p. 5080-5105.
16. Ajeel, R.K., W.-I. Salim, and K. Hasnan, *Experimental and numerical investigations of convection heat transfer in corrugated channels using alumina nanofluid under a turbulent flow regime.* Chemical Engineering Research and Design, 2019. **148**: p. 202-217.
17. Ajeel, R.K., W.-I. Salim, and K. Hasnan, *Thermal performance comparison of various corrugated channels using nanofluid: Numerical study.* Alexandria Engineering Journal, 2019. **58**(1): p. 75-87.
18. Ajeel, R.K., W.-I. Salim, and K. Hasnan, *Numerical investigations of heat transfer enhancement in a house shaped-corrugated channel: Combination of nanofluid and geometrical parameters.* Thermal Science and Engineering Progress, 2020. **17**: p. 100376.
19. Bhattad, A., J. Sarkar, and P. Ghosh, *Improving the performance of refrigeration systems by using nanofluids: A comprehensive review.* Renewable and Sustainable Energy Reviews, 2018. **82**: p. 3656-3669.
20. Umavathi, J.C., et al., *Unsteady two-fluid flow and heat transfer in a horizontal channel.* Heat and Mass Transfer, 2005. **42**(2): p. 81-90.
21. Awais, M., et al., *Computational assessment of Nano-particulate (Al2O3/Water) utilization for enhancement of heat transfer with varying straight section lengths in a serpentine tube heat exchanger.* Thermal Science and Engineering Progress, 2020. **20**: p. 100521.

22. Awais, M., et al., *Heat transfer and pressure drop performance of Nanofluid: A state-of-the-art review.* International Journal of Thermofluids, 2021. **9**: p. 100065.
23. Ajeel, R.K., et al., *Analysis of thermal-hydraulic performance and flow structures of nanofluids across various corrugated channels: An experimental and numerical study.* Thermal Science and Engineering Progress, 2020. **19**: p. 100604.
24. Bhattad, A., J. Sarkar, and P. Ghosh, *Exergetic analysis of plate evaporator using hybrid nanofluids as secondary refrigerant for low-temperature applications.* International Journal of Exergy, 2017. **24**(1): p. 1-20.
25. VeeraKrishna, M., G. Subba Reddy, and A. Chamkha, *Hall effects on unsteady MHD oscillatory free convective flow of second grade fluid through porous medium between two vertical plates.* Physics of fluids, 2018. **30**(2): p. 023106.
26. Chamkha, A.J., *Flow of two-immiscible fluids in porous and nonporous channels.* J. Fluids Eng., 2000. **122**(1): p. 117-124.
27. Dogonchi, A., et al., *Numerical simulation of hydrothermal features of Cu–H2O nanofluid natural convection within a porous annulus considering diverse configurations of heater.* Journal of Thermal Analysis and Calorimetry, 2020. **141**(5): p. 2109-2125.
28. Bayomy, A.M. and M. Saghir, *Experimental study of using γ-Al2O3–water nanofluid flow through aluminum foam heat sink: comparison with numerical approach.* International Journal of Heat and Mass Transfer, 2017. **107**: p. 181-203.
29. Goodarzi, M., et al., *Investigation of heat transfer and pressure drop of a counter flow corrugated plate heat exchanger using MWCNT based nanofluids.* International communications in heat and mass transfer, 2015. **66**: p. 172-179.
30. Goodarzi, M., et al., *Investigation of heat transfer performance and friction factor of a counter-flow double-pipe heat exchanger using nitrogen-doped, graphene-based nanofluids.* International Communications in Heat and Mass Transfer, 2016. **76**: p. 16-23.
31. Akhavan-Behabadi, M., et al., *An experimental investigation on rheological properties and heat transfer performance of MWCNT-water nanofluid flow inside vertical tubes.* Applied Thermal Engineering, 2016. **106**: p. 916-924.
32. Chamkha, A.J., T. Groşan, and I. Pop, *Fully developed free convection of a micropolar fluid in a vertical channel.* International Communications in Heat and Mass Transfer, 2002. **29**(8): p. 1119-1127.
33. Kumar, J.P., et al., *Fully-developed free-convective flow of micropolar and viscous*

fluids in a vertical channel. Applied Mathematical Modelling, 2010. **34**(5): p. 1175-1186.

34. Khoshvaght-Aliabadi, M. and A. Alizadeh, *An experimental study of Cu–water nanofluid flow inside serpentine tubes with variable straight-section lengths.* Experimental Thermal and Fluid Science, 2015. **61**: p. 1-11.
35. Feizabadi, A., M. Khoshvaght-Aliabadi, and A.B. Rahimi, *Numerical investigation on Al2O3/water nanofluid flow through twisted-serpentine tube with empirical validation.* Applied Thermal Engineering, 2018. **137**: p. 296-309.
36. Abed, W.M., et al., *Experimental investigation of the impact of elastic turbulence on heat transfer in a serpentine channel.* Journal of Non-Newtonian Fluid Mechanics, 2016. **231**: p. 68-78.
37. Ajeel, R.K., et al., *Turbulent convective heat transfer of silica oxide nanofluid through corrugated channels: An experimental and numerical study.* International Journal of Heat and Mass Transfer, 2019. **145**: p. 118806.
38. Ajeel, R.K., W.-I. Salim, and K. Hasnan, *Influences of geometrical parameters on the heat transfer characteristics through symmetry trapezoidal-corrugated channel using SiO2-water nanofluid.* International Communications in Heat and Mass Transfer, 2019. **101**: p. 1-9.
39. Huminic, G. and A. Huminic, *Heat transfer and entropy generation analyses of nanofluids in helically coiled tube-in-tube heat exchangers.* International Communications in Heat and Mass Transfer, 2016. **71**: p. 118-125.
40. Perwez, A., S. Shende, and R. Kumar, *Heat transfer and friction factor characteristic of spherical and inclined teardrop dimple channel subjected to forced convection.* Experimental Heat Transfer, 2019. **32**(2): p. 159-178.
41. Chen, J., H. Müller-Steinhagen, and G.G. Duffy, *Heat transfer enhancement in dimpled tubes.* Applied thermal engineering, 2001. **21**(5): p. 535-547.
42. García, A., et al., *The influence of artificial roughness shape on heat transfer enhancement: Corrugated tubes, dimpled tubes and wire coils.* Applied Thermal Engineering, 2012. **35**: p. 196-201.
43. Bhattad, A. and J. Sarkar, *Hydrothermal performance of plate heat exchanger with an alumina–graphene hybrid nanofluid: experimental study.* Journal of the Brazilian Society of Mechanical Sciences and Engineering, 2020. **42**(7): p. 1-10.
44. Bhattad, A., *Exergy analysis of plate heat exchanger with graphene alumina hybrid nanofluid: experimentation.* International Journal of Exergy, 2020. **33**(3): p. 254-262.

45. Kumar, P., et al., *Experimental investigation of heat transfer enhancement and fluid flow characteristics in a protruded surface heat exchanger tube.* Experimental Thermal and Fluid Science, 2016. **71**: p. 42-51.
46. Bhattad, A., J. Sarkar, and P. Ghosh, *Energy-economic analysis of plate evaporator using brine-based hybrid nanofluids as secondary refrigerant.* International Journal of Air-Conditioning and Refrigeration, 2018. **26**(01): p. 1850003.
47. Bhattad, A., J. Sarkar, and P. Ghosh, *Energetic and exergetic performances of plate heat exchanger using brine-based hybrid nanofluid for milk chilling application.* Heat Transfer Engineering, 2019.
48. Bhattad, A., J. Sarkar, and P. Ghosh, *Experimentation on effect of particle ratio on hydrothermal performance of plate heat exchanger using hybrid nanofluid.* Applied Thermal Engineering, 2019. **162**: p. 114309.
49. Bhattad, A., *Experimental investigation of Al2O3–MgO hot hybrid nanofluid in a plate heat exchanger*. Heat Transfer, 2020. **49**(4): p. 2344-2354.
50. Parvin, S., et al., *Thermal conductivity variation on natural convection flow of water–alumina nanofluid in an annulus.* International Journal of Heat and Mass Transfer, 2012. **55**(19-20): p. 5268-5274.
51. Sundar, L.S., et al., *Hybrid nanofluids preparation, thermal properties, heat transfer and friction factor–a review.* Renewable and Sustainable Energy Reviews, 2017. **68**: p. 185-198.
52. Crosser, R.L.H.a.O.K., *Thermal Conductivity of Heterogeneous Two-Component Systems.* Ind. Eng. Chem. Fundamen. 1962, , 1962. **1, 3, 187–191**.
53. Takabi, B. and H. Shokouhmand, *Effects of Al 2 O 3–Cu/water hybrid nanofluid on heat transfer and flow characteristics in turbulent regime.* International Journal of Modern Physics C, 2015. **26**(04): p. 1550047.
54. Suresh, S., et al., *Synthesis of Al2O3–Cu/water hybrid nanofluids using two step method and its thermo physical properties.* Colloids and Surfaces A: Physicochemical and Engineering Aspects, 2011. **388**(1-3): p. 41-48.
55. Saghir, M. and M. Rahman, *Forced convection of Al2O3–Cu, TiO2–SiO2, FWCNT–Fe3O4, and ND–Fe3O4 hybrid nanofluid in porous media.* Energies, 2020. **13**(11): p. 2902.
56. Sundar, L.S., M.K. Singh, and A.C. Sousa, *Enhanced heat transfer and friction factor of MWCNT–Fe3O4/water hybrid nanofluids.* International Communications in Heat and Mass Transfer, 2014. **52**: p. 73-83.

57. Sundar, L.S., et al., *Nanodiamond-Fe3O4 nanofluids: preparation and measurement of viscosity, electrical and thermal conductivities.* International Communications in Heat and Mass Transfer, 2016. **73**: p. 62-74.
58. Xuan, Y. and W. Roetzel, *Conceptions for heat transfer correlation of nanofluids.* International Journal of heat and Mass transfer, 2000. **43**(19): p. 3701-3707.
59. Lee, S., et al., *Measuring thermal conductivity of fluids containing oxide nanoparticles.* 1999.
60. Maiga, S.E.B., et al., *Heat transfer enhancement by using nanofluids in forced convection flows.* International journal of heat and fluid flow, 2005. **26**(4): p. 530-546.
61. Toghraie, D., et al., *Two-phase investigation of water-Al2O3 nanofluid in a micro concentric annulus under non-uniform heat flux boundary conditions.* International Journal of Numerical Methods for Heat & Fluid Flow, 2019.
62. Chamkha, A.J., *Unsteady laminar hydromagnetic fluid–particle flow and heat transfer in channels and circular pipes.* International Journal of Heat and Fluid Flow, 2000. **21**(6): p. 740-746.
63. Albojamal, A. and K. Vafai, *Analysis of single phase, discrete and mixture models, in predicting nanofluid transport.* International Journal of Heat and Mass Transfer, 2017. **114**: p. 225-237.
64. Kandasamy, R., N.A. bt Adnan, and R. Mohammad, *Nanoparticle shape effects on squeezed MHD flow of water based Cu, Al2O3 and SWCNTs over a porous sensor surface.* Alexandria Engineering Journal, 2018. **57**(3): p. 1433-1445.
65. Chamkha, A.J., *Hydromagnetic two-phase flow in a channel.* International journal of engineering science, 1995. **33**(3): p. 437-446.
66. Kim, D., et al., *Convective heat transfer characteristics of nanofluids under laminar and turbulent flow conditions.* Current Applied Physics, 2009. **9**(2): p. e119-e123.
67. Wen, D. and Y. Ding, *Experimental investigation into convective heat transfer of nanofluids at the entrance region under laminar flow conditions.* International journal of heat and mass transfer, 2004. **47**(24): p. 5181-5188.
68. Armaghani, T., et al., *MHD mixed convection of localized heat source/sink in an Al2O3-Cu/water hybrid nanofluid in L-shaped cavity.* Alexandria Engineering Journal, 2021. **60**(3): p. 2947-2962.
69. Kolsi, L., et al., *Numerical investigation of combined buoyancy-thermocapillary convection and entropy generation in 3D cavity filled with Al2O3 nanofluid.* Alexandria Engineering Journal, 2017. **56**(1): p. 71-79.

70. Awais, M., et al., *Synthesis, heat transport mechanisms and thermophysical properties of nanofluids: A critical overview.* International Journal of Thermofluids, 2021. **10**: p. 100086.
71. Ahmed, F., et al., *Computational assessment of thermo-hydraulic performance of Al2O3-water nanofluid in hexagonal rod-bundles subchannel.* Progress in Nuclear Energy, 2021. **135**: p. 103700.
72. Izadi, M., A. Behzadmehr, and D. Jalali-Vahida, *Numerical study of developing laminar forced convection of a nanofluid in an annulus.* International journal of thermal sciences, 2009. **48**(11): p. 2119-2129.
73. Kumar, A., R. Maithani, and A.R.S. Suri, *Numerical and experimental investigation of enhancement of heat transfer in dimpled rib heat exchanger tube.* Heat and Mass Transfer, 2017. **53**(12): p. 3501-3516.
74. Yadigaroglu, G., et al., *Trends and needs in experimentation and numerical simulation for LWR safety.* Nuclear Engineering and Design, 2003. **221**(1-3): p. 205-223.
75. Rahimi-Esbo, M. and Y. Vazifeshenas, *Comparison of thermo-hydraulic performance of nanofluids and mixing vanes in a triangular fuel rod bundle.* Journal of the Brazilian Society of Mechanical Sciences and Engineering, 2015. **37**(1): p. 173-186.
76. *Fluent, I., et al., 2006. Fluent 6.3 user's guide*. 2006: Fluent documentation.
77. Ahmed, H.E., B. Salman, and A.S. Kerbeet, *Heat transfer enhancement of turbulent forced nanofluid flow in a duct using triangular rib.* International Journal of Heat and Mass Transfer, 2019. **134**: p. 30-40.
78. Ahmed, F., et al., *Thermohydraulic performance of water mixed Al2O3, TiO2 and graphene-oxide nanoparticles for nuclear fuel triangular subchannel.* Thermal Science and Engineering Progress, 2021. **24**: p. 100929.
79. Yakhot, V. and S.A. Orszag, *Renormalization group analysis of turbulence. I. Basic theory.* Journal of scientific computing, 1986. **1**(1): p. 3-51.
80. Versteeg, H.K. and W. Malalasekera, *An introduction to computational fluid dynamics: the finite volume method*. 2007: Pearson education.
81. Benaissa, K., et al., *Predicting initial erosion during the hole erosion test by using turbulent flow CFD simulation.* Applied Mathematical Modelling, 2012. **36**(8): p. 3359-3370.
82. Bianco, V., O. Manca, and S. Nardini, *Performance analysis of turbulent convection heat transfer of Al2O3 water-nanofluid in circular tubes at constant wall temperature.* Energy, 2014. **77**: p. 403-413.

83. Karale, C.M., S.S. Bhagwat, and V.V. Ranade, *Flow and heat transfer in serpentine channels.* AIChE Journal, 2013. **59**(5): p. 1814-1827.
84. Rao, Y., et al., *Experimental and numerical study of heat transfer and flow friction in channels with dimples of different shapes.* Journal of Heat Transfer, 2015. **137**(3).
85. Lewis, M., *Optimising the thermohydraulic performance of rough surfaces.* international Journal of Heat and Mass transfer, 1975. **18**(11): p. 1243-1248.
86. Bhattad, A. and J. Sarkar, *Effects of nanoparticle shape and size on the thermohydraulic performance of plate evaporator using hybrid nanofluids.* Journal of Thermal Analysis and Calorimetry, 2021. **143**(1): p. 767-779.
87. Bhattad, A., J. Sarkar, and P. Ghosh, *Heat transfer characteristics of plate heat exchanger using hybrid nanofluids: effect of nanoparticle mixture ratio.* Heat and Mass Transfer, 2020. **56**(8): p. 2457-2472.